Research Square

Preprints are preliminary reports that have not undergone peer review.
They should not be considered conclusive, used to inform clinical practice,
or referenced by the media as validated information.

Spatiotemporal Variability of Defined Extreme and Convective Rainfall in Sabah Malaysia from 2000 to 2024 Using GPM IMERG and JAXA GSMaP

Franky Herman
ds21@iluv.ums.edu.my
Universiti Malaysia Sabah (UMS)
Justin Sentian
Universiti Malaysia Sabah (UMS)
Nurrul Fazlina Osman
Universiti Malaysia Sabah (UMS)
Jackson Hian Wui Chang
Universiti Malaysia Sabah (UMS)
Maggie Chel Gee Ooi
National University of Malaysia (UKM)
Ju Neng Liew
National University of Malaysia (UKM)
Miklin Ationg
Jabatan Pengairan dan Saliran

Research Article

Keywords: extreme rainfall, convective rainfall, Sabah, GPM, Jaxa, monsoon

Posted Date: November 11th, 2026

DOI: https://doi.org/10.21203/rs.3.rs-11397111/v1

License: This work is licensed under a Creative Commons Attribution 4.0 International License.
Read Full License

Additional Declarations: No competing interests reported.

Spatiotemporal Variability of Defined Extreme and Convective Rainfall in Sabah Malaysia from 2000 to 2024 Using GPM IMERG and JAXA GSMaP

Franky Herman[1*], Justin Sentian[1†], Nurrul Fazlina Osman[1†], Jackson Hian Wui Chang[2†], Maggie Chel Gee Ooi[3†], Ju Neng Liew[4†], Miklin Ationg[5†]

[1*]Climate Change Research Laboratory, Faculty of Science and Technology, Universiti Malaysia Sabah (UMS), UMS Road, Kota Kinabalu, 88400, Sabah, Malaysia.
[2]Faculty of Science and Technology, Universiti Malaysia Sabah (UMS), UMS Road, Kota Kinabalu, 88400, Sabah, Malaysia.
[3]Centre of Tropical Climate Change System, Institute of Climate Change, National University of Malaysia (UKM), Bangi, 43600, Selangor, Malaysia.
[4]Department of Earth Sciences and Environment, Faculty of Sciences and Technology, National University of Malaysia (UKM), Bangi, 43600, Selangor, Malaysia.
[5]Department of Irrigation and Drainage (DID), Sabah, Jalan Tasik Luyang Off, Jalan Maktab Gaya, Kota Kinabalu, 88767, Sabah, Malaysia.

*Corresponding author(s). E-mail(s):
franky_herman_ds21@iluv.ums.edu.my; jsentian@ums.edu.my;
Contributing authors: jsentian@ums.edu.my;
nurrulfazlina.osman@ums.edu.my; jacksonchw@ums.edu.my;
chelgee.ooi@ukm.edu.my; juneng@ukm.my;
Miklin.Ationg@sabah.gov.my;
†These authors contributed equally to this work.

Abstract

Short-duration high-intensity rainfall poses substantial challenges for hydroclimatic hazard assessment in tropical regions, yet its spatial, seasonal and temporal variability remains insufficiently characterised across Sabah, Malaysian Borneo. This study characterises threshold-defined extreme and convective rainfall occurrence across Sabah during 2000–2024 and evaluates its consistency between GPM and JAXA in relation to monsoon seasons and large-scale climate variability. Rainfall occurrences were identified using operational thresholds adopted from Malaysia's Department of Irrigation and Drainage and analysed at hourly resolution on a common 0.1° grid. Frequencies were evaluated during the Northeast Monsoon (NEM) and Southwest Monsoon (SWM) across 27 administrative districts grouped into five geographical Zones. The results reveal pronounced spatial and temporal heterogeneity, with the Sandakan and Kudat Zones repeatedly exhibiting relatively high rainfall-occurrence frequencies across multiple five-year periods. Sandakan was particularly prominent during the SWM, whereas Kudat showed greater prominence during the NEM. Convective rainfall was generally more frequent and spatially extensive than hourly extreme rainfall. GPM and JAXA broadly agreed on the recurrent geographical concentration of rainfall occurrence but differed in its magnitude, spatial extent and temporal evolution, particularly for extreme rainfall. Inter-product correlations were sparse and spatially fragmented for extreme rainfall but more extensive for convective rainfall, particularly during the NEM. Comparisons with ENSO, the Indian Ocean Dipole and the Madden–Julian Oscillation showed no consistent correspondence between individual climate phases and periods of enhanced rainfall frequency, indicating that these large-scale modes alone do not explain the observed variability. Overall, the study provides a 25-year spatially explicit baseline of threshold-defined rainfall occurrence across Sabah, identifies the Sandakan and Kudat Zones as recurrent high-frequency areas, and demonstrates the importance of accounting for satellite-product uncertainty when assessing short-duration rainfall variability and associated hazards.

Keywords: extreme rainfall, convective rainfall, Sabah, GPM, Jaxa, monsoon

1 Introduction

Anthropogenic climate change alters the characteristics of weather and climate extremes, increasing concerns about changes in their frequency, intensity, and spatial distribution [1]. In tropical regions such as Malaysia, precipitation variability is further shaped by monsoonal circulation, inter-annual climate variability, and convective pro-cesses, resulting in pronounced spatial and temporal heterogeneity [2-3]. Characterising the spatial and temporal variability of extreme rainfall is therefore important for improving understanding of hydro-climatic hazards and supporting climate resilience and disaster risk management.

Although an increasing number of studies have examined extreme rainfall in Malaysia, extreme events are commonly identified using percentile-based or other standardized statistical thresholds in daily intervals that facilitate comparison across

global and regional climate datasets [4-11]. Such approaches are particularly common in climate-model-based assessments, where standardized indices enable comparisons between historical simulations and future projections [12-17]. While these definitions are valuable for assessing relative changes in rainfall extremes, they may not correspond directly to thresholds adopted in national or operational assessments of hazardous rainfall in Malaysia, including those applied by the Department of Irrigation and Drainage (DID) Malaysia and the Malaysian Meteorological Department (Met Malaysia).

Rain-gauge and other ground-based observations provide detailed information at individual locations but may have limited capacity to resolve rainfall heterogeneity across regions characterised by complex topography and uneven observational coverage [9,18]. Satellite precipitation products provide a complementary source of spatially continuous rainfall observations and therefore offer an opportunity to examine rainfall variability across Sabah using locally relevant operational thresholds [19]. However, long-term, dis-trict-resolved assessments of sub-daily extreme and convective rainfall frequency across Sabah using such thresholds remain limited, particularly in determining whether recur-rent spatial patterns are consistently represented across independent satellite precipitation products.

This need is particularly relevant in Sabah, where rainfall variability is associated with the Northeast and Southwest Monsoons (NEM and SWM), interannual variability related to the El Niño–Southern Oscillation (ENSO) and Indian Ocean Dipole (IOD), intra-seasonal variability associated with the Madden–Julian Oscillation (MJO), and regional convective processes [3, 20-24] Complex topography and land–sea interactions further contribute to pronounced spatial heterogeneity across the state [10, 25-26]. In this study, extreme and convective rainfall are treated as operationally distinct rainfall characteristics: extreme rainfall is defined by high hourly rainfall intensity, whereas the convective-rainfall criterion represents high rainfall accumulation over continuous short-duration periods [27]. These locally relevant threshold-based definitions provide a framework for identifying potentially hazardous rainfall occurrences at sub-daily time-scales [19, 28-29]. However, their representation may vary among satellite precipitation products because of differences in observational characteristics, retrieval algorithms, and sensitivity to short-duration high-intensity precipitation.

Therefore, the primary objective of this study is to characterise the spatial and seasonal frequency of threshold-defined extreme and convective rainfall across Sabah during 2000–2024, with particular emphasis on identifying districts and geographic zones that repeatedly exhibit relatively high rainfall frequencies. The analysis covers Sabah's 27 administrative districts and five geographic zones during the NEM and SWM, while temporal variations in rainfall frequency are compared descriptively with ENSO, IOD, and MJO conditions to provide large-scale climatic context. Rather than validating or ranking satellite-product performance, the inter-product comparison is used to distinguish recur-rent rainfall-frequency characteristics from those that are product-dependent. The study thereby provides a 25-year spatially explicit baseline of operationally defined extreme and convective rainfall frequency and identifies recurrent rainfall-prone regions relevant to hydro-climatic risk assessment in Sabah.

2 Methodology

2.1 Study Domain and Temporal Frame

This study examines the spatial and temporal variability of extreme and convective rainfall frequency across Sabah(northern Borneo), Malaysia (Figure 1), over the 25-year period from 2000 to 2024. Sabah is characterised by complex topography, extensive coastal areas, and a tropical maritime climate that contribute to substantial spatial variability in rainfall[25]. To characterise this variability at an administrative scale, the analysis was conducted across Sabah's 27 districts, grouped into five geographic zones: the Westcoast Zone (Papar, Putatan, Penampang, Kota Kinabalu, Tuaran, Kota Belud, and Ranau); Interior Zone (Tambunan, Keningau, Beaufort, Tenom, Pensiangan, Sipitang, and Kuala Penyu); Kudat Zone (Kudat, Kota Marudu, and Pitas); Sandakan Zone (Telupid, Beluran, Tongod, Kinabatangan, and Sandakan); and Tawau Zone (Lahad Datu, Kunak, Semporna, Tawau, and Kalabakan). These administrative groupings were used to summarize and compare rainfall-event frequencies among districts and broader geographic regions of Sabah.

2.2 Datasets

2.2.1 Precipitation datasets

The Hourly precipitation data from the Global Precipitation Measurement (GPM) Integrated Multi-satellite Retrievals for GPM (IMERG) Final Run Version 07 [30] and the Japan Aerospace Exploration Agency (JAXA) Global Satellite Mapping of Precipitation (GSMaP) Hourly Version 8 [31] were used to characterise extreme and convective rainfall frequency across Sabah, Malaysia, from 2000 to 2024. Both products have a nominal spatial resolution of 0.1° and were regridded to a common 0.1° spatial grid to ensure spatial correspondence between their rainfall-frequency estimates. The products were analysed independently using the same rainfall-event definitions and temporal aggregation procedures. GPM half-hourly precipitation estimates were aggregated to an hourly time step following [32] whereas JAXA data were retained at their original hourly temporal resolution. The resulting datasets were aligned spatially and temporally before the rain-fall-frequency indices were calculated.

2.2.2 Climate index datasets

Three large-scale climate indices were used to provide climatic context for the temporal variability of extreme and convective rainfall frequency: the El Niño–Southern Oscillation (ENSO), Indian Ocean Dipole (IOD) and Madden–Julian Oscillation (MJO). ENSO variability was represented by the Oceanic Niño Index (ONI), which measures sea-surface temperature anomalies in the region. ONI data were obtained from the NOAA National Centers for Environmental Information (NCEI) via Our World in Data (https://ourworldindata.org/). IOD variability was represented by the Dipole Mode Index (DMI), obtained from the NASA Jet Propulsion Laboratory (JPL) Sea Level Portal (https://sealevel.jpl.nasa.gov/overlay-iod/). Intraseasonal variability

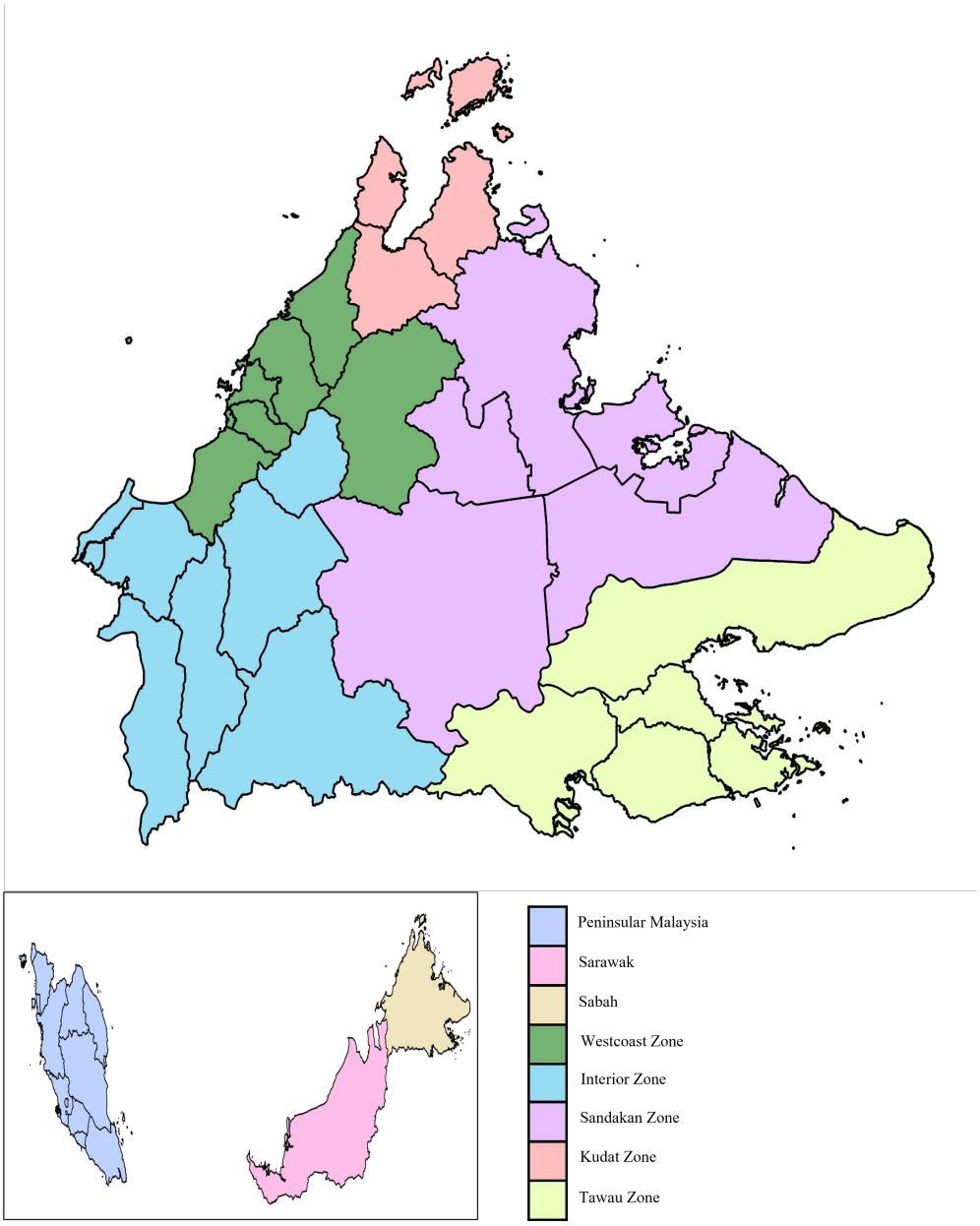


Fig. 1 Study area and zonal division of Sabah

associated with the MJO was represented by the Real-time Outgoing Longwave Radiation MJO Index (ROMI), obtained from the NOAA Physical Sciences Laboratory (PSL; https://psl.noaa.gov/).

The ONI and DMI phases were classified according to the criteria specified by their respective data sources. Individual MJO events were identified using the ROMI criteria, which define an event as a local maximum in index amplitude within a centred 30-day period that exceeds one standard deviation. The ROMI phase classification follows the convention of the Real-time Multivariate MJO (RMM) index and comprises eight phases. In this study, MJO phases 2–7 were considered, with phases 4 and 5 receiving particular attention because of their stronger association with rainfall variability, following [21-24]. The climate indices and identified MJO events were compared descriptively with temporal variations in rainfall-event frequency to identify periods of correspondence between large-scale climate variability and rainfall-frequency fluctuations.[33] This comparison was intended to provide climatic context and explore potential associations rather than quantify statistical relationships or establish causal links.

2.3 Threshold-Based Rainfall Indices

Rather than applying percentile-based rainfall indices, this study adopted threshold-based criteria derived from operational rainfall classifications used by the Department of Irrigation and Drainage (DID) Malaysia (online available at https://publicinfobanjir.water.gov.my/hujan/data-hujan/?lang=en). The two rainfall indices were evaluated at common 0.1° grid cell:

1. **Extreme Hourly Rainfall Index (I_{EHR}):** An occurrence was recorded when hourly precipitation intensity exceeded $60\,\mathrm{mm\,h^{-1}}$ during any hour of a day.
2. **Convective Rainfall Index (I_{CR}):** An occurrence was identified when cumulative rainfall exceeded 60 mm over a continuous period of 2–4 hours.

Both indices were evaluated using hourly precipitation records from 2000 to 2024. For the extreme rainfall index, a grid cell was assigned one occurrence for a day if at least one hourly precipitation value exceeded the threshold. For the cumulative rainfall index, continuous 2–4 hour accumulation windows were evaluated within each 24-hour day. If one or more windows exceeded the cumulative threshold, the grid cell was assigned one occurrence for that day, irrespective of the number of qualifying or overlapping windows.

Consequently, the resulting frequencies represent the number of days meeting each threshold criterion, rather than the number of individual hours or qualifying accumulation windows. Convective-rainfall frequency was expected to be equal to or greater than extreme-rainfall frequency because the 2–4 hour cumulative criterion can be satisfied by rainfall events that do not exceed the hourly extreme threshold. Accordingly, differences in frequency between the two indices primarily reflect their different accumulation timescales rather than independent differences in rainfall occurrence

2.4 Monsoonal Seasonal Aggregation

Rainfall-event frequencies and climate indices were aggregated according to the two principal monsoon seasons affecting Sabah: The Southwest Monsoon (SWM; May–September) and the Northeast Monsoon (NEM; November–March) [21,34]. April and October were excluded from the seasonal analysis because they represent inter-monsoon transition periods. The two seasons were analysed separately to examine differences in the spatial and temporal distributions of extreme and convective rainfall across Sabah. The final NEM period was limited to November–December 2024 since the GPM dataset used in this study ended in December 2024.

For each rainfall index and satellite precipitation product, monthly event frequencies were summed across the months defining each monsoon season to obtain seasonal event frequencies at each grid cell. The SWM was assigned to the calendar year in which it occurred, whereas the NEM was identified by the year in which the season began, generally spanning November of that year to March of the following year. All NEM seasons prior to the final study year were aggregated over November–March, whereas the final NEM record comprised November–December 2024, consistent with the temporal endpoint of the GPM dataset. This approach enabled consistent inter-product comparisons over their common period of record.

2.5 Variability Analysis

2.5.1 Zonal-Statistic and District-level Analysis

For each district, the maximum grid-cell rainfall-event frequency was extracted separately for each rainfall index, satellite product and monsoon season. These maxima were used to identify districts containing localised high-frequency rainfall hotspots and to compare their occurrence frequencies among Sabah's 27 districts. The maximum grid-cell frequency was selected to represent localised hotspot occurrence rather than district-average rainfall conditions.

2.5.2 Spatio-Temporal Frequency Patterns

For each rainfall index, satellite product and monsoon season, grid-cell frequencies were averaged across the five corresponding seasons within each five-year period. The resulting maps were used to examine changes in the spatial distribution of rainfall-event frequency between successive periods. District-level statistics and grid-cell maps of mean rainfall-event frequency provided complementary perspectives, identifying localised hotspots at the district level and illustrating the spatial distribution of mean rainfall-event frequency across Sabah.

Spatial patterns of temporal correspondence between GPM and JAXA were assessed using Spearman's rank correlation coefficient (ρ). Spearman's ρ was calculated independently at each 0.1° grid cell using the corresponding seasonal rainfall-frequency series from GPM and JAXA. The resulting spatial distribution of ρ was used to identify areas where the two satellite products exhibited similar or dissimilar temporal variations in rainfall-event frequency. Statistical significance was assessed at $p < 0.05$, and non-significant or undefined correlations were masked.

3 Results

3.1 Zonal Variability of Extreme and Convective Rainfall Frequency

Seasonal extreme- and convective-rainfall frequencies exhibited pronounced spatial and temporal variability across Sabah's five geographic zones and 27 administrative districts (Figures 2 and 3). Both satellite products showed substantial year-to-year variability, although the timing and magnitude of higher-frequency periods differed between GPM and JAXA. GPM showed several periods of elevated rainfall frequency, particularly between 2000 –2015, whereas JAXA showed comparatively elevated frequencies during several later periods after 2015. These differences indicate product-dependent temporal characteristics rather than a consistent temporal trend.

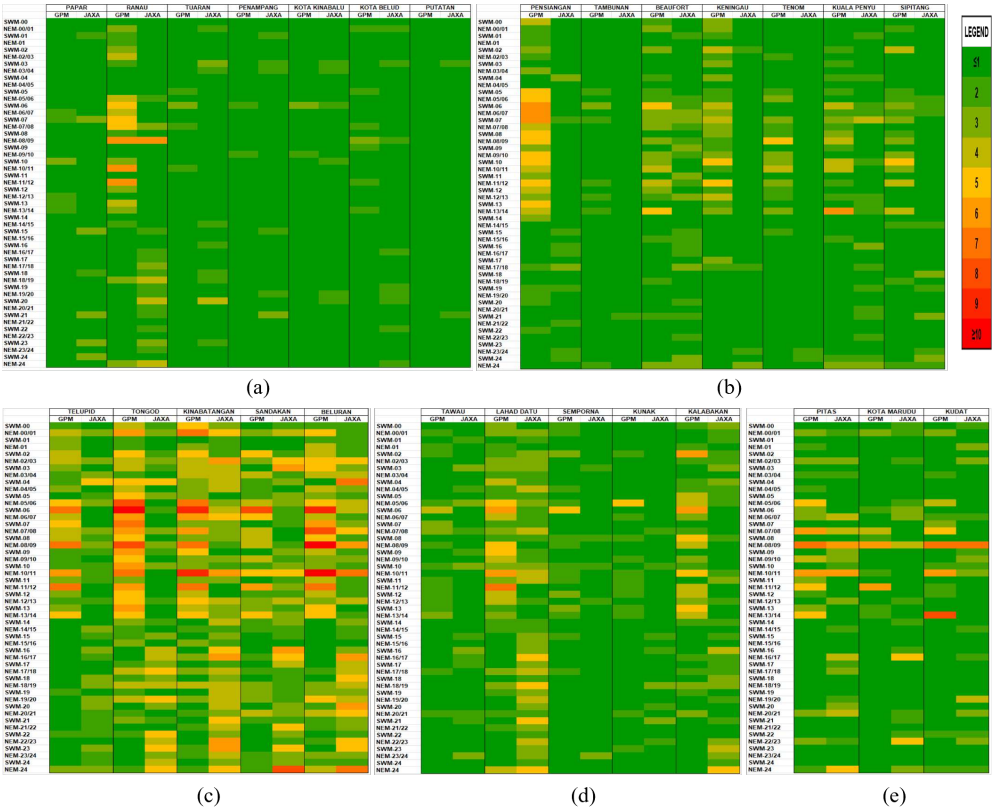


Fig. 2 Heatmap of extreme rainfall frequency across regional zones and administrative districts in Sabah: (a) Westcoast Zone, (b) Interior Zone, (c) Sandakan Zone, (d) Tawau Zone, and (e) Kudat Zone.

The Westcoast Zone generally exhibited less pronounced temporal variability in extreme-rainfall frequency, with most districts recording approximately 2–6 occurrences per monsoon season (Figure 2). Ranau recorded comparatively higher frequencies, whereas most other districts generally experienced approximately 1–3 occurrences per season. A similar range was observed across the Interior Zone, although Pensiangan exhibited relatively higher frequencies during several monsoon seasons between 2005 to 2015. The remaining Interior districts generally exhibited lower extreme-rainfall frequencies during the later part of the study period.

The Sandakan Zone exhibited greater spatial and temporal variability, with extreme-rainfall frequencies generally ranging from approximately 2–7 occurrences per monsoon season. Relatively high frequencies were evident across the districts within the Sandakan Zone during several monsoon seasons between 2000 and 2014. In the Tawau Zone, most districts recorded approximately 2–5 occurrences per monsoon season, with Lahad Datu exhibiting comparatively higher frequencies and greater temporal variability. The Kudat Zone also showed substantial differences among districts, with extreme-rainfall frequencies varying across monsoon seasons and between the two satellite products.

Convective rainfall occurred more frequently than extreme rainfall across all five geo-graphic zones, with frequencies ranging from approximately up to 20 occurrences per monsoon season (Figure 3). Though the event is less frequent observed in JAXA, ranging approximately 2 to 14 occurrences and noticeable onward 2014. The Westcoast Zone generally exhibited lower spatio-temporal variability in convective-rainfall frequency, although Papar and Ranau experienced several periods of relatively high frequency, reaching approximately 10–20 occurrences per season. The Interior, Tawau, and Kudat Zones also showed considerable temporal variability, with relatively high frequencies generally ranging from approximately 6–16 occurrences per season. Elevated frequencies occurred intermittently across districts within these zones, although Tambunan, Semporna, and Kunak generally exhibited lower frequencies than the more prominent districts within their respective zones.

The Sandakan Zone exhibited the highest and most persistent maximum grid-cell convective-rainfall frequencies among the five geographical Zones. Frequencies generally ranged from approximately 2–18 occurrences per monsoon season, while all districts within the Zone experienced repeated periods of elevated convective-rainfall frequency. During several monsoon seasons, frequencies reached approximately 14 to more than 20 occurrences. Overall, the district-level results demonstrate that both extreme- and convective-rainfall frequencies varied substantially across Sabah, with the Sandakan Zone consistently exhibiting greater rainfall frequency and temporal variability than most other geographic zones.

3.2 Spatio-temporal Variability of Extreme Frequency

The five-year seasonal-mean frequency distributions revealed pronounced spatial and temporal variability in extreme and convective rainfall occurrence across Sabah during the SWM and NEM (Figures 4 and 5). Although the spatial extent and mean frequency distributions varied between GPM and JAXA and across all the five-year periods, both products repeatedly identified the Kudat and Sandakan Zones as regions of relatively

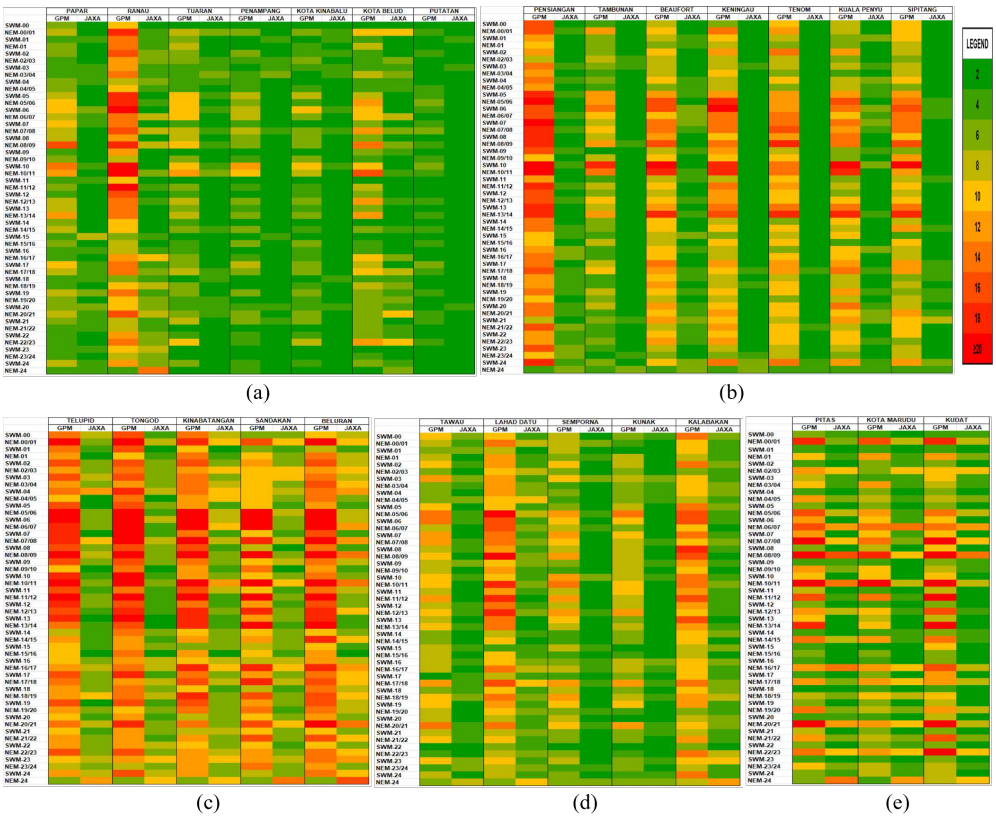


Fig. 3 Heatmap of convective rainfall frequency across regional zones and administrative districts in Sabah: (a) Westcoast Zone, (b) Interior Zone, (c) Sandakan Zone, (d) Tawau Zone, and (e) Kudat Zone.

high rainfall-occurrence frequency, particularly for convective rainfall. This spatial prominence showed a seasonal contrast, with relatively high frequencies recurring in the Kudat Zone during the NEM and in the Sandakan Zone during the SWM across multiple five-year periods.

For extreme rainfall, GPM did not identify a clearly recurrent high-frequency area across the five-year periods during the SWM (Figure 4). During the NEM, however, recurrent extreme-rainfall occurrence was evident around Beluran during 2005–2009 and 2010–2014. JAXA exhibited a different spatial pattern, with extreme-rainfall frequencies of approximately one occurrence day per season extending across parts of the Sandakan Zone during the SWM in multiple periods. During the NEM, JAXA more consistently identified extreme-rainfall occurrence within the Kudat and Sandakan Zones across the five-year periods, with localised seasonal-mean frequencies reaching approximately two occurrence days per season in the highest-frequency areas. Differences between GPM and JAXA were therefore evident in both the spatial extent and

temporal persistence of extreme-rainfall occurrence, although both products broadly identified Kudat and Sandakan Zone as recurrent areas of relatively elevated frequency.

Convective rainfall was considerably more spatially extensive than extreme rainfall and exhibited pronounced variability between satellite products, monsoon seasons and five-year periods (Figure 5). Relatively high seasonal-mean frequencies repeatedly occurred within the Kudat and Sandakan Zones, with localised frequencies approaching five occurrence days per season during some five-year periods. Areas of elevated frequency were also evident within parts of the Interior Zone, although their spatial persistence was less consistent than that observed in the Kudat and Sandakan Zones. The Sandakan Zone remained particularly prominent across multiple periods and in both satellite products.

Inter-product differences in convective-rainfall occurrence were more apparent during the SWM, when GPM and JAXA differed in both the spatial extent and location of elevated-frequency areas. During the NEM, the two products showed broader agreement in the regional distribution of convective-rainfall occurrence across multiple five-year periods, particularly over the same zone. Nevertheless, differences in the magnitude and spatial extent of elevated-frequency areas remained apparent between GPM and JAXA.

Overall, the spatial patterns demonstrate that threshold-defined rainfall-occurrence frequencies were not uniformly distributed across Sabah. The repeated prominence of the Sandakan and Kudat Zones across multiple five-year periods and in both satellite, products indicate a recurrent regional concentration of relatively high rainfall-occurrence frequency. This spatial consistency was particularly evident for convective rainfall, although its seasonal expression differed between regions. Nevertheless, differences between GPM and JAXA, particularly during the SWM, indicate that the detailed spatial representation of extreme and convective rainfall occurrence remains product dependent.

The Spearman correlation analysis revealed limited and spatially heterogeneous temporal correspondence between GPM and JAXA for extreme-rainfall frequency (Figure 6). During the SWM, positive correlations were sparse and confined to isolated areas, indicating limited temporal correspondence between the two products at those grid cells. During the NEM, positive correlations were more apparent, particularly across parts of the Kudat and Sandakan Zones, although their spatial distribution remained fragmented.

In contrast, spatially more extensive temporal correspondence was evident for convective-rainfall frequency. During the SWM, positive correlations were more widely distributed than for extreme rainfall, with coefficients of approximately 0.4–0.6 occurring across parts of the Westcoast and Tawau Zones. During the NEM, correlations of approximately 0.4–0.6 became more spatially extensive, particularly across the Kudat, Sandakan and Interior Zones. Localised areas of stronger correlation were also evident, although these remained spatially discontinuous. Overall, GPM and JAXA exhibited more spatially extensive temporal correspondence for convective-rainfall frequency than for extreme-rainfall frequency, particularly during the NEM.

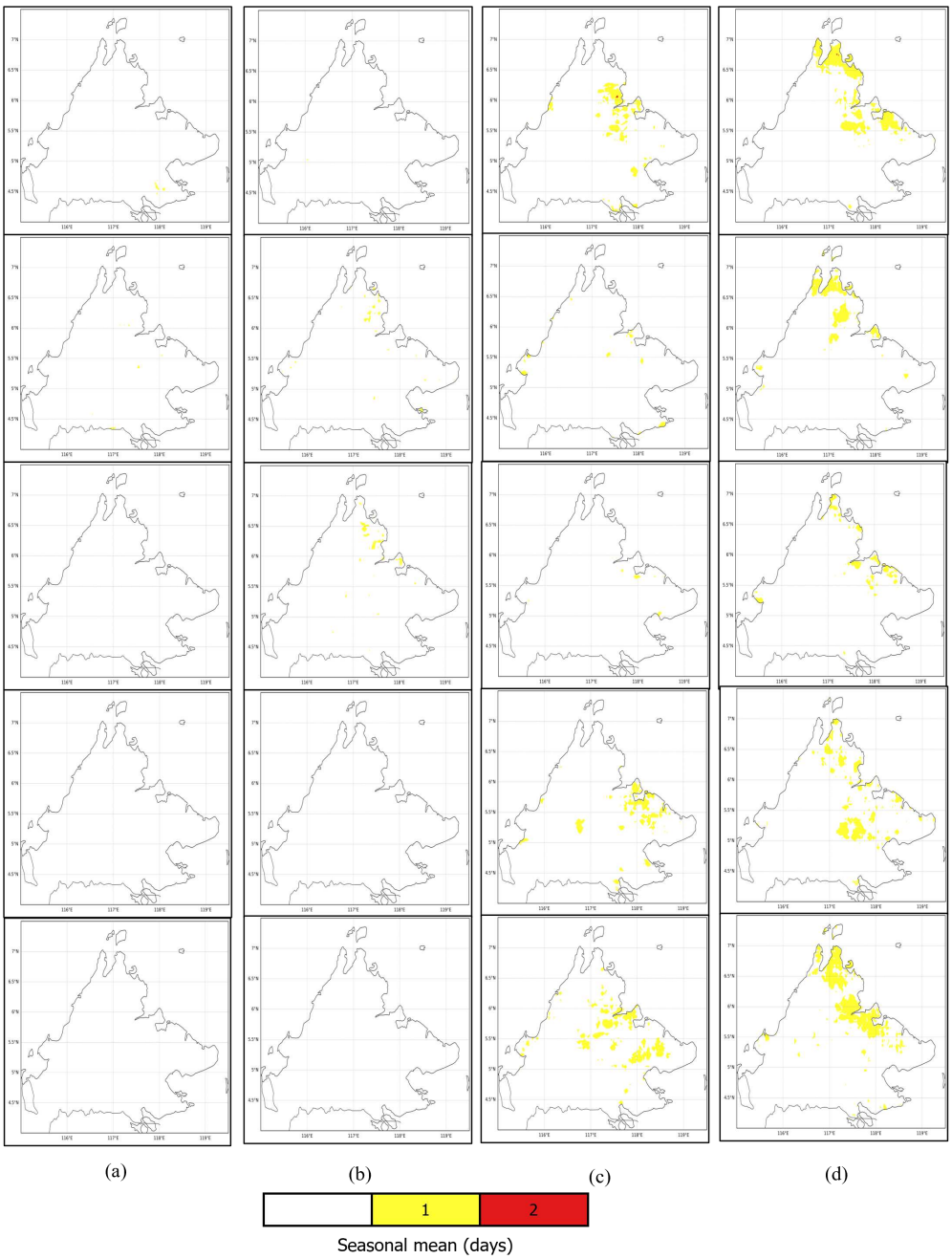


Fig. 4 Spatial mean frequency for extreme rainfall in Sabah across five-year periods of 2000-2004 first row, 2005-2009 second row, 2010-2014 third row, 2015-2019 fourth row and 2020-2024 fifth row during SWM and NEM based on GPM (a–b) and JAXA (c–d) satellite precipitation products.

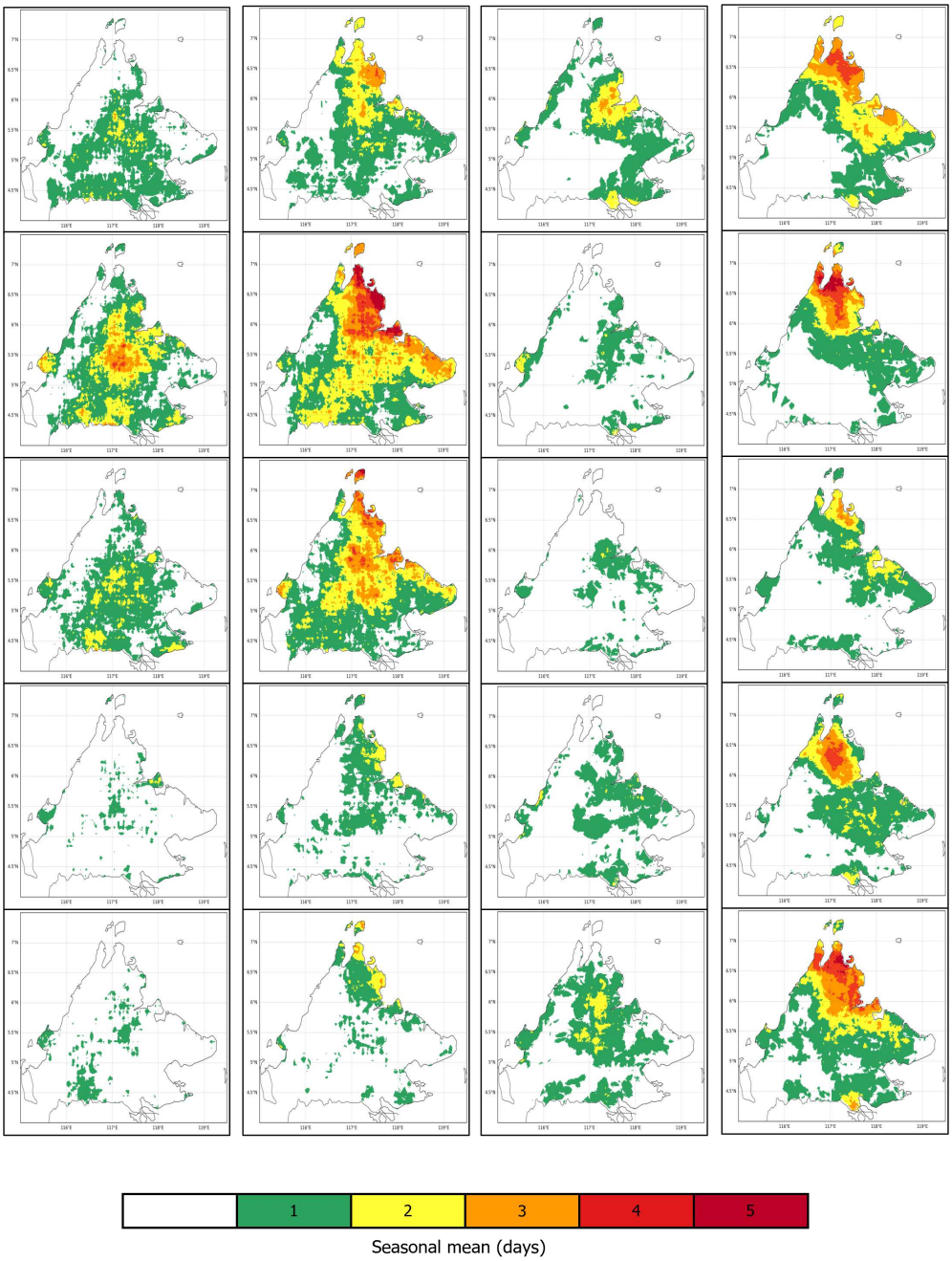


Fig. 5 Spatial mean frequency for convective rainfall in Sabah across five-year periods of 2000-2004 first row, 2005-2009 second row, 2010-2014 third row, 2015-2019 fourth row and 2020-2024 fifth row during SWM and NEM based on GPM (a–b) and JAXA (c–d) satellite precipitation products.

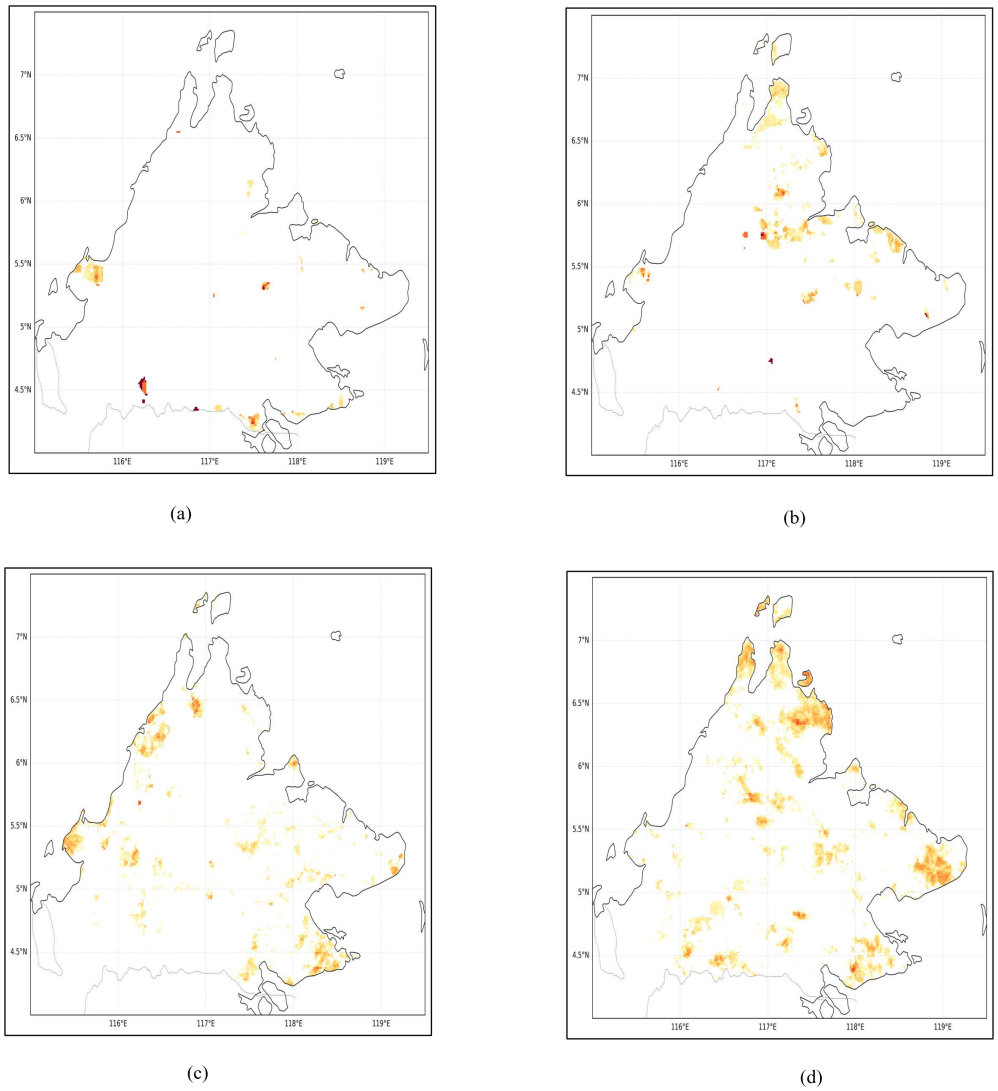


Fig. 6 Spatial distribution of Spearman's rank correlation coefficient (ρ) between the seasonal rainfall-frequency time series of GPM and JAXA for extreme rainfall during (a) SWM and (b) NEM, and convective rainfall during (c) SWM and (d) NEM. Grid cells with non-significant ($p < 0.05$) or undefined correlations are masked.

4 Discussion

The repeated prominence of the Sandakan and Kudat Zones across multiple five-year periods indicates that high rainfall occurrence is regionally concentrated rather than uniformly distributed. Sandakan was therefore selected for detailed temporal assessment be-cause of its persistent spatial prominence and pronounced variability across monsoon seasons and satellite products (Figure 7 and 8). Result for the rest of zones are provided in Appendix A (Figures A1–A4). Convective-rainfall occurrences were generally more frequent and spatially extensive than hourly extreme-rainfall occurrences. This difference likely reflects the cumulative 2–4 hr criterion, which can capture sustained or successive rainfall accumulation without requiring an individual hour to exceed 60 mm/hr [35-37]. However, this operational definition should not be interpreted as a direct diagnosis of convective storm processes. The higher occurrence frequency of convective rainfall should not necessarily be interpreted as indicating greater hazard severity, as the two indices represent different rainfall characteristics and thresholds. The recurrent hotspots in Sandakan and Kudat may help prioritise areas for rainfall monitoring and further investigation, although the frequency patterns do not predict individual events or independently establish flood risk.

The recurrent high frequencies over the Sandakan and Kudat Zones are physically consistent with interactions between the monsoonal circulation and Sabah's coastal and topographic environment. Moist maritime flow, coastal convergence and orographic lifting can enhance moisture convergence and atmospheric ascent, providing favourable conditions for intense and persistent rainfall [38-40]. The seasonal differences further indicate modulation by the monsoonal background, with the greater prominence of Kudat during the NEM potentially associated with enhanced moisture transport and low-level convergence under northeasterly flow, whereas the prominence of Sandakan during the SWM suggests a different interaction between regional circulation and local geographical controls.

The temporal analysis further shows that large-scale climate variability does not provide a simple explanation for rainfall-frequency fluctuations in Sabah. Some period of elevated frequencies coincided with La Niña and negative IOD conditions, particularly during parts of 2005–2009 and 2010–2014, whereas other rainfall peaks occurred under different ENSO–IOD configurations. Similarly, several peaks coincided with MJO phases 3–7, but the correspondence was not consistent across geographical zones or satellite products. ENSO, IOD and MJO should therefore be regarded as potential modulators rather than deterministic controls of rainfall occurrence. Their influence is likely conditioned by the pre-vailing monsoonal circulation, regional moisture availability and mesoscale processes, which may explain the heterogeneous rainfall responses reported here and in previous studies over Borneo [21,25,33,34, 41-45]

The findings of this study complement those of [25,46] who highlighted the sporadic timing and locations of heavy rainfall in East Malaysia [10], who identified non-stationarity in yearly extreme rainfall across East Malaysia. Together, these studies and the present findings highlight the spatial and temporal heterogeneity of extreme rainfall, which is reflected in its sporadic occurrence, recurrent hotspots and temporal variability across Sa-bah. Differences between GPM and JAXA further demonstrate that estimated rainfall frequencies are sensitive to the satellite product used [47-48],

while differences in rainfall definitions and analytical methods may also influence comparisons between studies. These findings emphasise the importance of considering spatial and temporal variability, methodological differences and product-dependent uncertainties when characterising extreme rainfall [49-51]. Nevertheless, identifying recurrent hotspots does not enable the prediction of individual rainfall events.

An important finding is that the inferred rainfall-frequency characteristics also depend on the satellite product. GPM and JAXA broadly identified recurrent high-frequency regions in Kudat and Sandakan, but differed in the magnitude, spatial extent and temporal evolution of rainfall occurrence. This disagreement was particularly evident for extreme rainfall, including the reduction in GPM-derived frequency after approximately 2014–2015 that was not consistently reproduced by JAXA. Differences in retrieval algorithms, temporal sampling and the representation of short-duration high-intensity rainfall can influence whether the extreme threshold is exceeded [52-55]. Consistent with these concerns, [47,52, 56-58] found that GMP and JAXA products varied in performance across precipitation intensities and had limitations in detecting extreme precipitation events. Consequently, product-specific temporal changes should not be interpreted as climatic trends without independent observational validation and formal trend analysis.

The Spearman analysis reinforces this distinction between the two rainfall criteria. Extreme rainfall showed sparse and spatially fragmented inter-product correlations, indicating limited consistency between GPM and JAXA in reproducing variability in seasonal rainfall frequency. In contrast, convective rainfall exhibited more spatially extensive inter-product temporal correspondence, particularly during the NEM, with correlations of approximately 0.4–0.6 across several parts of Sabah. The greater correspondence for cumulative rainfall may reflect its potentially lower sensitivity to differences in retrieving isolated hourly intensity maxima, whereas small differences in the magnitude or timing of intense rainfall can determine whether the hourly threshold is exceeded [59-62]. Thus, while GPM and JAXA show agreement in the broad geographical concentration of rainfall occurrence, their agreement is weaker for the temporal behaviour of short-duration extreme events.

Overall, this study demonstrates that threshold-defined high-intensity rainfall occurrence in Sabah is characterised by recurrent regional hotspots and substantial temporal and inter-product variability. The Sandakan and Kudat Zones emerge as prominent areas of re-current rainfall occurrence, while descriptive comparisons reveal no consistent relation-ships with ENSO, the IOD or the MJO. These findings suggest that rainfall variability may reflect interactions among large-scale climate modes, monsoonal circulation and regional geographical processes. Differences between GPM and JAXA further highlight the sensitivity of estimated rainfall frequencies to the satellite product and rainfall-event definition. Several limitations warrant consideration. The absence of independent rain-gauge validation limits the assessment of product-specific uncertainties, while the descriptive comparison with climate indices does not establish statistically significant relationships or causal effects. Future research should validate satellite-derived estimates against ground observations, apply formal statistical analyses to investigate climate relationships and temporal trends, and integrate rainfall data with catchment characteristics and flood records to better assess implications for flood risk.

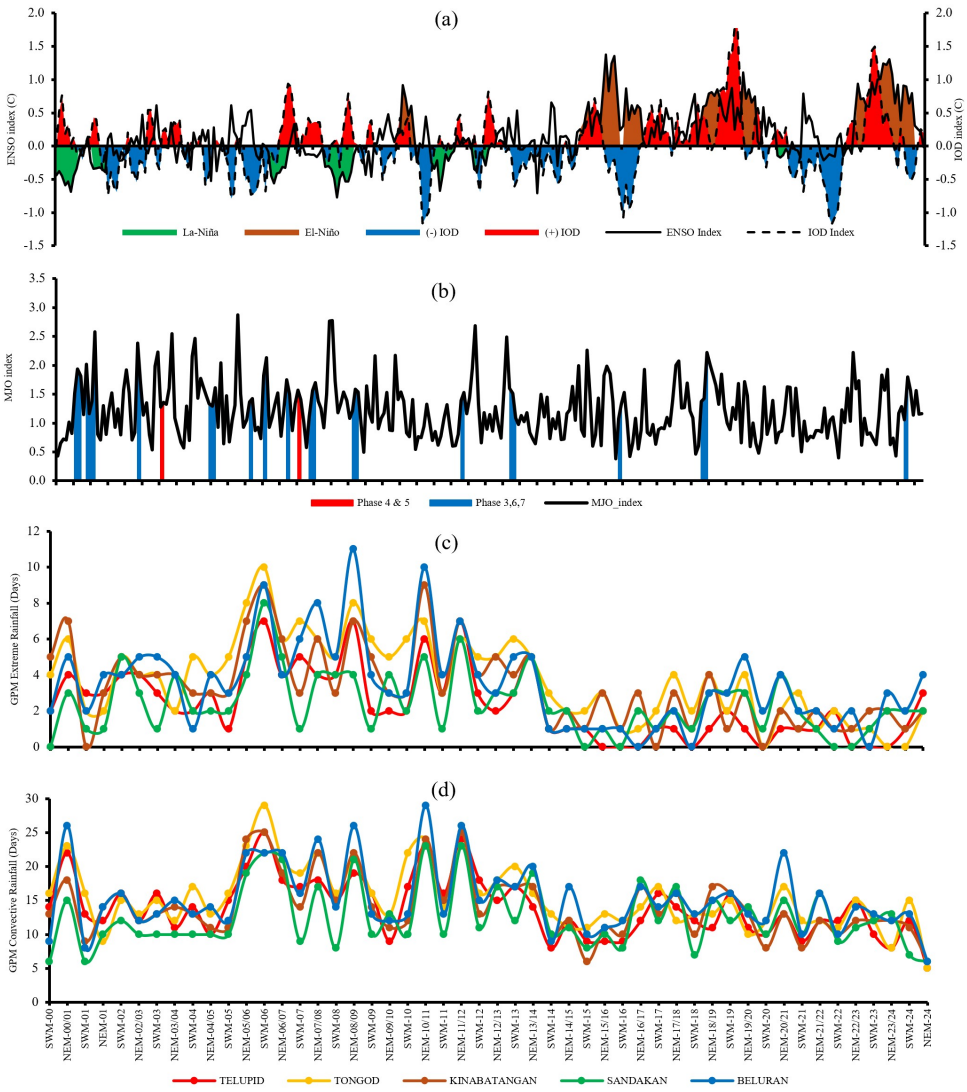


Fig. 7 Temporal extreme variability frequency across the Sandakan Zone, Sabah, in relation to (a) ENSO and IOD and (b) MJO phases conditions during 2000–2024, based on GPM (c) for extreme and (d) for convective precipitation.

5 Conclusion

This study characterised the spatial and temporal variability of threshold-defined extreme and convective rainfall frequency across Sabah during 2000–2024 and assessed the consistency of these patterns between GPM and JAXA in relation to monsoon

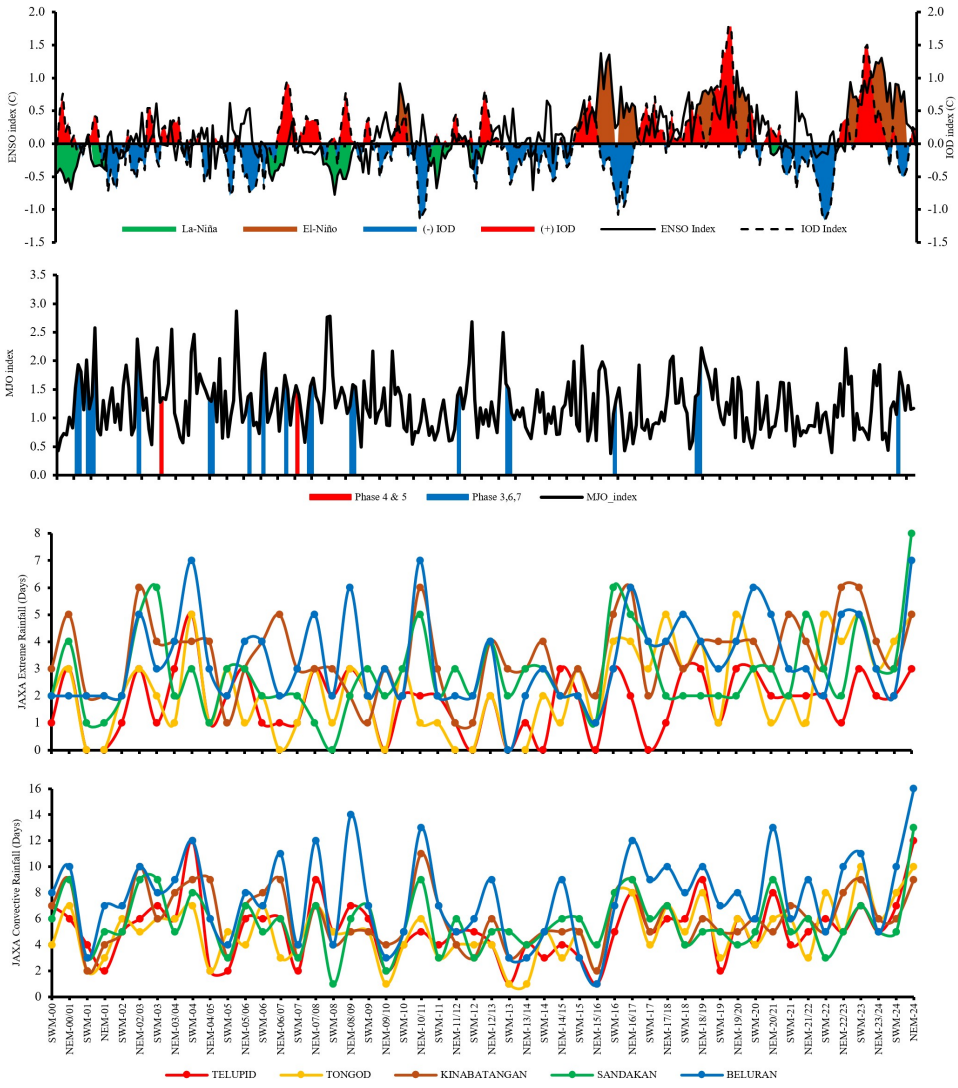


Fig. 8 Temporal extreme variability frequency across the Sandakan Zone, Sabah, in relation to (a) ENSO and IOD and (b) MJO phases conditions during 2000–2024, based on JAXA (c) for extreme and (d) for convective precipitation.

seasons and large-scale climate variability. The results demonstrate substantial spatial and temporal heterogeneity, with the Sandakan and Kudat Zones repeatedly emerging as areas of relatively high rainfall-occurrence frequency across multiple five-year periods. Seasonal differences were also evident, with the Sandakan Zone showing greater prominence during the SWM and the Kudat Zone during the NEM. Convective rainfall was generally more frequent and spatially extensive than hourly extreme

rainfall, demonstrating the importance of the temporal criterion used to characterise high-intensity rainfall occurrence.

Despite broad agreement in identifying recurrent high-frequency Zones, GPM and JAXA differed in the magnitude, spatial extent and temporal variability of rainfall occurrence. This inter-product difference was particularly evident for extreme rainfall, whereas convective rainfall showed broader temporal agreement between the products, especially during the NEM. The temporal comparison with ENSO, IOD and MJO further showed that periods of enhanced rainfall frequency were not consistently associated with particular phases of these climate modes. Their influence on rainfall occurrence in Sabah is therefore unlikely to operate independently of the prevailing monsoonal and regional atmospheric conditions.

Overall, the findings establish that rainfall-frequency variability across Sabah is characterised by recurrent spatial concentrations but considerable seasonal, temporal and in-ter-product variability. The persistent identification of the Sandakan and Kudat Zones provides a spatial basis for prioritising further investigation of high-intensity rainfall and associated hazards, while the differences between GPM and JAXA highlight the need to consider satellite-product uncertainty when interpreting short-duration rainfall extremes. The 25-year spatially explicit assessment presented here therefore provides a baseline for subsequent observational validation, process-based investigation and assessment of rain-fall-related hazards and climate resilience across Sabah.

Acknowledgements. During the preparation of this manuscript, the authors used OpenAI to assist with language refinement and the formalisation of academic writing. The authors have reviewed and edited the output and take full responsibility for the content of this publication.

Declarations

Some journals require declarations to be submitted in a standardised format. Please check the Instructions for Authors of the journal to which you are submitting to see if you need to complete this section. If yes, your manuscript must contain the following sections under the heading 'Declarations':

- Funding: This research received no external funding.
- Conflicts of Interest: The authors declare no conflicts of interest.
- Informed Consent Statement: Not applicable.
- Ethical Approval: Not applicable.
- Consent for publication: Not applicable.
- Data Availability Statement: The datasets analysed during the current study are available from the corresponding author on reasonable request.
- Materials availability: Not applicable
- Code availability: Not applicable
- Author Contributions: Conceptualization, F.H.; data curation, F.H.; formal analysis, F.H., J.S. and J.H.W.C.; investigation, F.H., J.S. and J.H.W.C.; methodology, F.H., M.C.G.O. and J.N.L.; project administration, F.H., N.F.O. and M.A.; resources, F.H., N.F.O. and M.A.; software, F.H. and M.C.G.O.; supervision,

J.S., J.H.W.C., M.C.G.O. and J.N.L.; validation, F.H., J.S., J.H.W.C., M.C.G.O. and J.N.L.; visualization, F.H.; writing—original draft preparation, F.H.; writing—review and ed-iting, F.H., J.S., J.H.W.C. and M.C.G.O. All authors have read and agreed to the published version of the manuscript.

Table 1 List of abbreviations.

Abbreviation	Definition
DID	Department of Irrigation and Drainage (Malaysia)
DMI	Dipole Mode Index
ENSO	El Niño–Southern Oscillation
GPM	Global Precipitation Measurement
GSMaP	Global Satellite Mapping of Precipitation
IMERG	Integrated Multi-satellitE Retrievals for GPM
IOD	Indian Ocean Dipole
JAXA	Japan Aerospace Exploration Agency
JPL	Jet Propulsion Laboratory
MJO	Madden–Julian Oscillation
NASA	National Aeronautics and Space Administration
NCEI	National Centers for Environmental Information
NEM	Northeast Monsoon
NOAA	National Oceanic and Atmospheric Administration
ONI	Oceanic Niño Index
PSL	Physical Sciences Laboratory
ROMI	Real-time Multivariate MJO Index
SWM	Southwest Monsoon
h	Hour
km	Kilometre
mm	Millimetre
mm h^{-1}	Millimetres per hour
ρ	Spearman's rank correlation coefficient

If any of the sections are not relevant to your manuscript, please include the heading and write 'Not applicable' for that section.

Editorial Policies for:

Springer journals and proceedings: https://www.springer.com/gp/editorial-policies

Nature Portfolio journals: https://www.nature.com/nature-research/editorial-policies

Scientific Reports: https://www.nature.com/srep/journal-policies/editorial-policies

BMC journals: https://www.biomedcentral.com/getpublished/editorial-policies

Appendix A Temporal extreme and convective variability frequency in relation to ENSO and IOD and MJO phases conditions during 2000–2024 for GPM JAXA for Westcoast Zone, Interior Zone, Tawau Zone, and Kudat Zone

References

[1] Seneviratne, S.I.; Zhang, X.; Adnan, M.; Badi, W.; Dereczynski, C.; Di Luca, A.; Ghosh, S.; Iskandar, I.; Kossin, J.; Lewis, S.; Otto, F.; Pinto, I.; Satoh, M.; Vicente-Serrano, S.M.; Wehner, M.; Zhou, B. Weather and Climate Extreme Events in a Changing Climate. In *Climate Change 2021: The Physical Science Basis. Contribution of Working Group I to the Sixth Assessment Report of the Intergovernmental Panel on Climate Change*; Masson-Delmotte, V., Zhai, P., Pirani, A., Connors, S.L., Péan, C., Berger, S., Caud, N., Chen, Y., Goldfarb, L., Gomis, M.I., Huang, M., Leitzell, K., Lonnoy, V., Matthews, J.B.R., Maycock, T.K., Waterfield, T., Yelekçi, O., Yu, R., Zhou, B., Eds.; Cambridge University Press: Cambridge, UK, 2021; pp. 1513–1766. https://doi.org/10.1017/9781009157896.013.

[2] Xiao, H.M.; Lo, M.H.; Yu, J.Y. The Increased Frequency of Combined El Niño and Positive IOD Events since the 1960s and Its Impacts on Maritime Continent Hydroclimates. *Sci. Rep.* **2022**, *12*, 7532. https://doi.org/10.1038/s41598-022-11663-1.

[3] Chang, J.H.W.; Ooi, M.C.G.; Liew, J.; Wong, Y.J.; Chee, F.P.; Sentian, J.; Aryastana, P.; Punay, J.P.; Lin, N.H. Equatorial Wave Embedded within the Madden–Julian Oscillation Leading to the 2021 Peninsular Malaysia Flood. *Meteorol. Atmos. Phys.* **2026**, *138*, 75. https://doi.org/10.1007/s00703-026-01162-7.

[4] Mayowa, O.O.; Pour, S.H.; Shahid, S.; Mohsenipour, M.; Harun, S.B.; Heryansyah, A.; Ismail, T. Trends in Rainfall and Rainfall-Related Extremes in the East Coast of Peninsular Malaysia. *J. Earth Syst. Sci.* **2015**, *124*, 1609–1622. https://doi.org/10.1007/s12040-015-0639-9.

[5] Wong, C.L.; Liew, J.; Yusop, Z.; Ismail, T.; Venneker, R.; Uhlenbrook, S. Rainfall Characteristics and Regionalization in Peninsular Malaysia Based on a High-Resolution Gridded Dataset. *Water* **2016**, *8*, 500. https://doi.org/10.3390/w8110500.

[6] Ng, C.Y.; Wan Jaafar, W.Z.; Mei, Y.; Othman, F.; Lai, S.H.; Liew, J. Assessing the Changes of Precipitation Extremes in Peninsular Malaysia. *Int J Climatol* **2022**, *42*, 7914–7937. https://doi.org/10.1002/joc.7684.

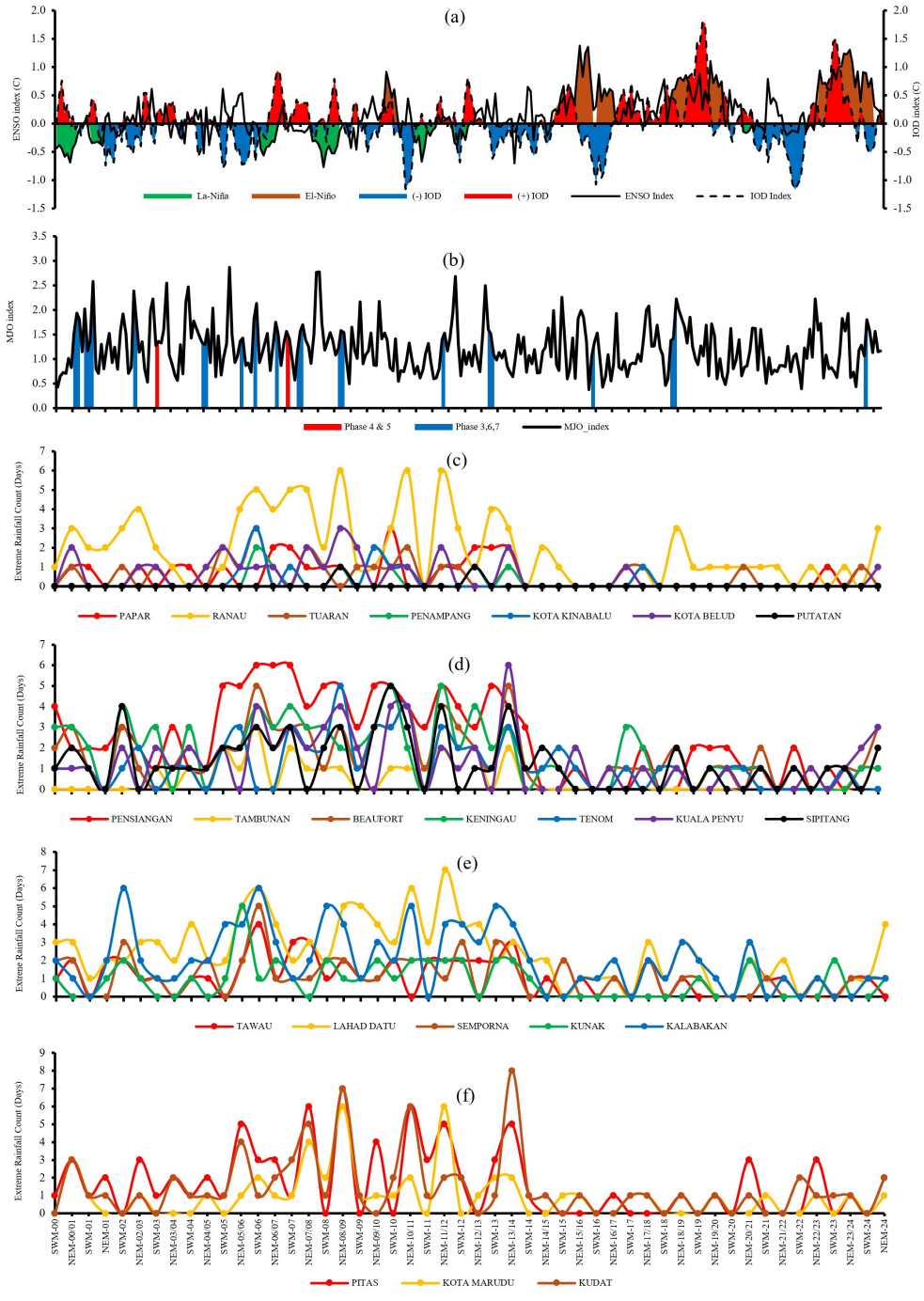


Fig. A1 Temporal extreme variability frequency in relation to (a) ENSO and IOD and (b) MJO phases conditions during 2000–2024 based on GPM for; (c) Westcoast Zone, (d) Interior Zone, (e) Tawau Zone, and (f) Kudat Zone.

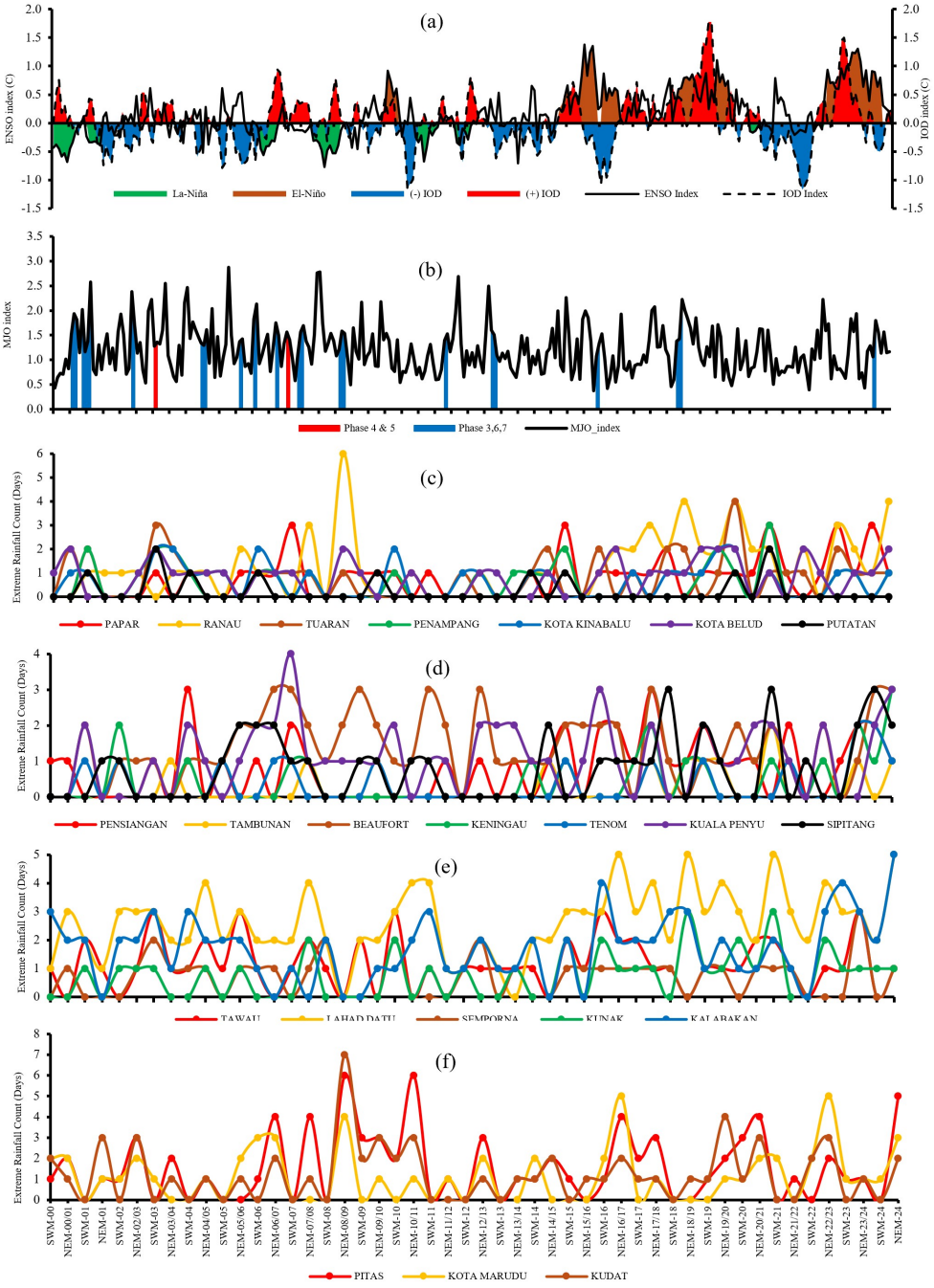


Fig. A2 Temporal extreme variability frequency in relation to (a) ENSO and IOD and (b) MJO phases conditions during 2000–2024 based on JAXA for; (c) Westcoast Zone, (d) Interior Zone, (e) Tawau Zone, and (f) Kudat Zone.

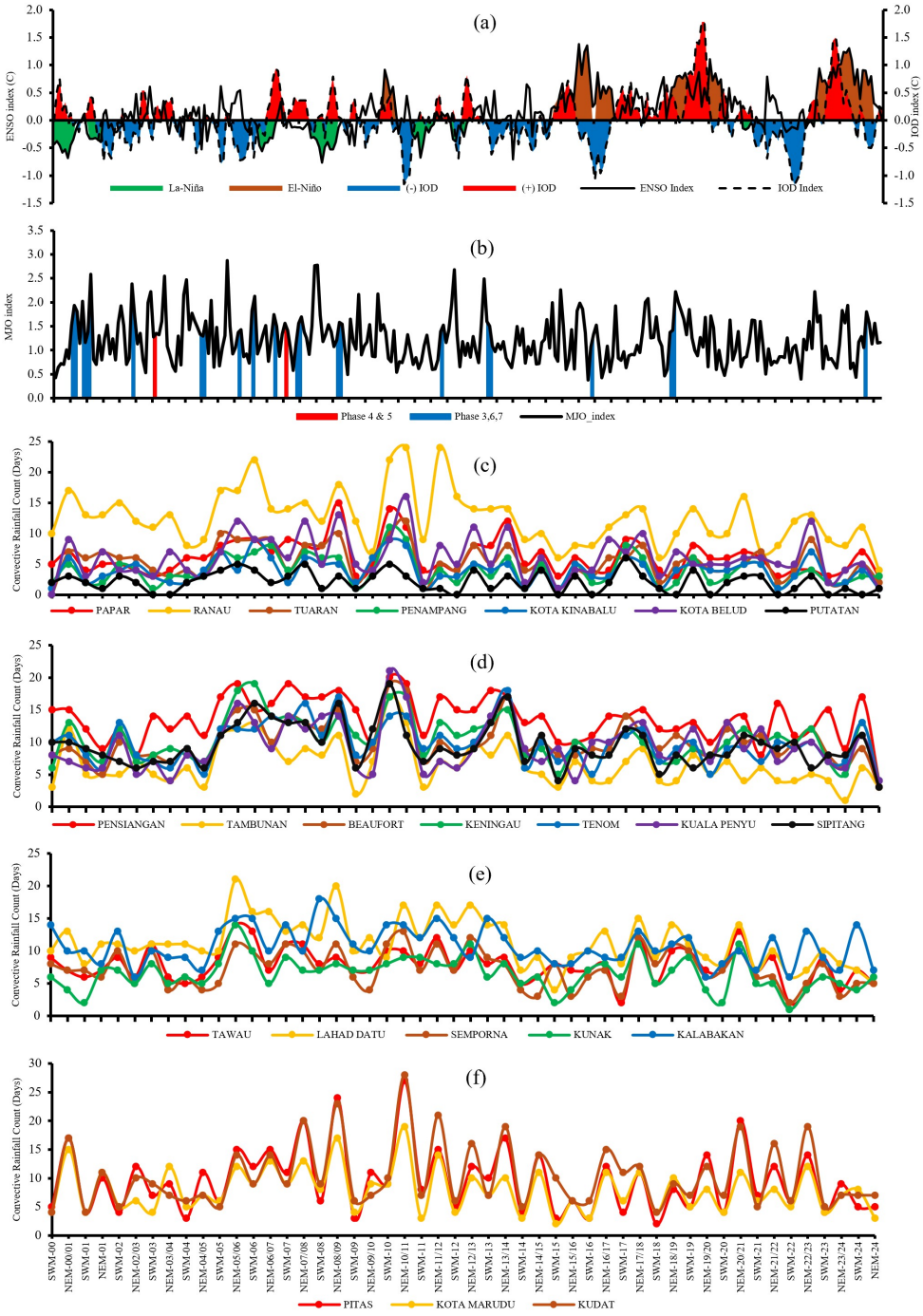


Fig. A3 Temporal convective variability frequency in relation to (a) ENSO and IOD and (b) MJO phases conditions during 2000–2024 based on GPM for; (c) Westcoast Zone, (d) Interior Zone, (e) Tawau Zone, and (f) Kudat Zone.

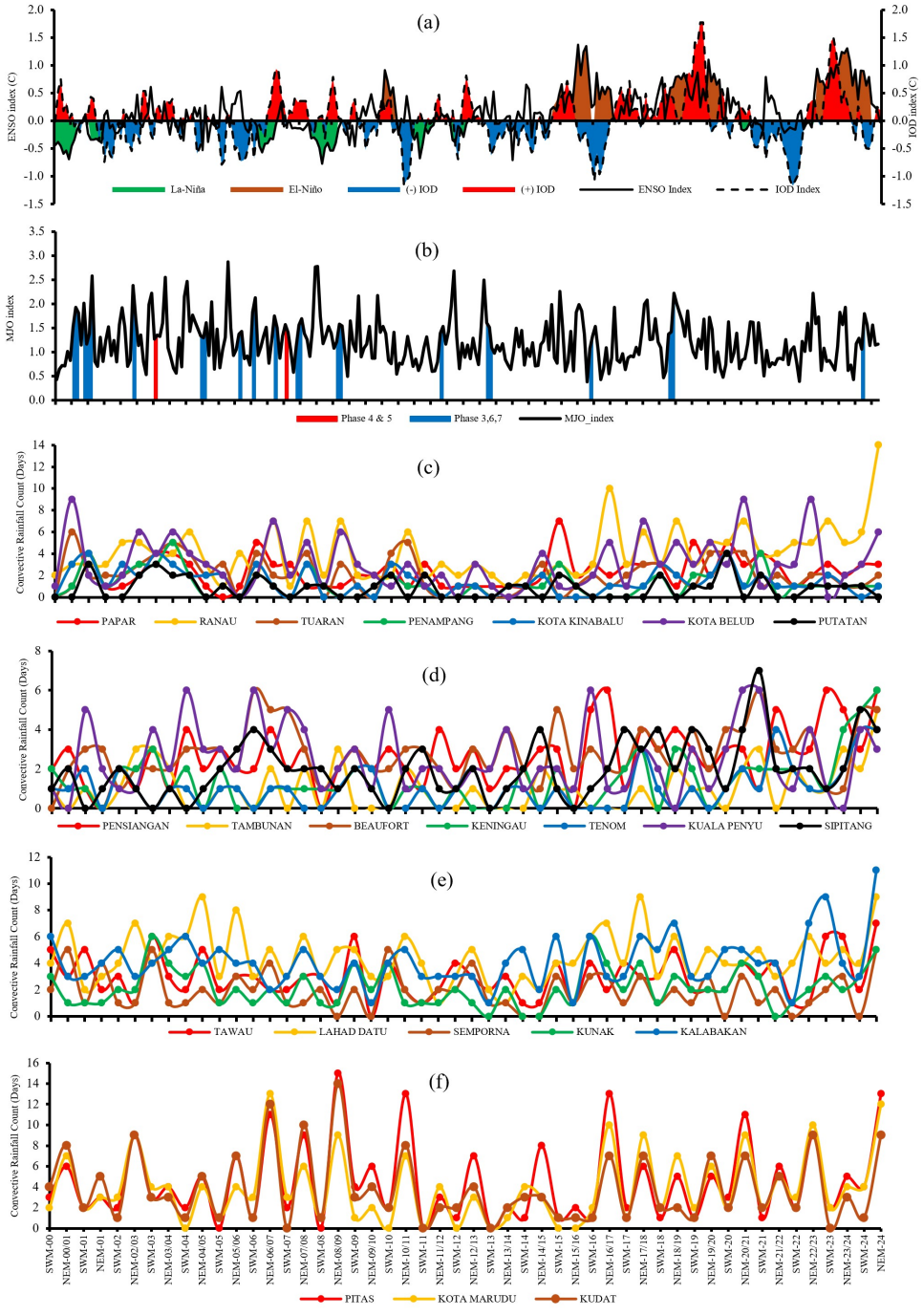


Fig. A4 Temporal convective variability frequency in relation to (a) ENSO and IOD and (b) MJO phases conditions during 2000–2024 based on JAXA for; (c) Westcoast Zone, (d) Interior Zone, (e) Tawau Zone, and (f) Kudat Zone.

[7] Ramadhan, R.; Muharsyah, R.; Marzuki; Yusnaini, H.; Vonnisa, M.; Hashiguchi, H.; Suryanto, W.; Sholihun. Evaluation of GPM IMERG products for extreme precipitation over Indonesia *J of Physics: IOP Publishing Conference Series ICRLP-2021* **2022**, *2309*, 012008. https://doi.org/10.1088/1742-6596/2309/1/012008

[8] 8. Sulaiman, N.A.F.; Shaharudin, S.M.; Ismail, S.; Zainuddin, N.H.; Tan, M.L.; Abd Jalil, Y. Predictive modelling of statistical downscaling based on hybrid machine learning model for daily rainfall in East-Coast Peninsular Malaysia. *Symmetry* **2022**, *14*, 927. https://doi.org/10.3390/sym14050927

[9] Noor, M.A.I.M.; Halek, M.A.; Lim, A.F.; Lim, M.R.; Ahmat, H. Rainfall Intensity Classification in the East Coast of Malaysia Using Discriminant Analysis. *J. Sustainability Sci. Manage.* **2023**, *18*(7), 87–102. https://doi.org/10.46754/jssm.2023.07.006.

[10] Ng, J.L.; Huang, Y.F.; Yong, S.L.S.; Lee, J.C.; Ahmed, A.N.; Mirzaei, M. Analysing the Variability of Non-Stationary Extreme Rainfall Events Amidst Climate Change in East Malaysia. *Aqua Water Infrastruct. Ecosyst. Soc.* **2024**, *73*(7), 1494–1509. https://doi.org/10.2166/aqua.2024.132.

[11] Alzian, N.A.; Chenoli, S.N.; Mohd Nor, M.F.F.; Jeong Yik, D.; Abu Samah, A. Spatial and Temporal Variability of Extreme Rainfall Events over Peninsular Malaysia. *Hydrol. Sci. J.* **2025**, *70*(8), 1365–1383. https://doi.org/10.1080/02626667.2025.2479106.

[12] Noor, M.; Ismail, T.; Shahid, S.; Nashwan, M.S.; Ullah, S. Development of Multi-Model Ensemble for Projection of Extreme Rainfall Events in Peninsular Malaysia. *Hydrol. Res.* **2019**, *50*(6), 1772–1788. https://doi.org/10.2166/nh.2019.097.

[13] Tangang, F.; Juneng, L.; Cruz, F.; Chung, J.X.; Ngai, S.T.; Salimun, E.; Mohd, M.S.F.; Santisirisomboon, J.; Singhruck, P.; PhanVan, T.; Ngo-Duc, T. Multi-Model Projections of Precipitation Extremes in Southeast Asia Based on CORDEX-Southeast Asia Simulations. *Environ. Res.* **2020**, *184*, 109350. https://doi.org/10.1016/j.envres.2020.109350.

[14] Ge, F.; Zhu, S.; Luo, H.; Zhi, X.; Wang, H. Future Changes in Precipitation Extremes over Southeast Asia: Insights from CMIP6 Multi-Model Ensemble. *Environ. Res. Lett.* **2021**, *16*(2), 024013. https://doi.org/10.1088/1748-9326/abd7ad.

[15] Sobh, M.T.; Hamed, M.M.; Nashwan, M.S.; Shahid, S. Future Projection of Bioclimatic Indicators over Southeast Asia Using CMIP6. *Sustainability* **2022**, *14*(20), 13596. https://doi.org/10.3390/su142013596.

[16] Chung, J.X.; Juneng, L.; Santisirisomboon, J.; Ngo-Duc, T.; Phan-Van, T.; Trinh Tuan, L.; Cruz, F.; Dado, J.; Srisawadwong, R.; Gunawan, D.; McGregor, J.L. Future Changes in Mean and Extreme Precipitation over Peninsular Malaysia Using CORDEX-SEA 5 km Simulations. *APN Sci. Bull.* **2023**, *13*(1), 1–10. https://doi.org/10.30852/sb.2023.2348.

[17] Liang, J.; Tan, M.L.; Catto, J.L.; Hawcroft, M.K.; Hodges, K.I.; Haywood, J.M. Projected Near-Term Changes in Monsoon Precipitation over Peninsular Malaysia in the HighResMIP Multi-Model Ensembles. *Clim. Dyn.* **2023**, *60*(3), 1151–1171. https://doi.org/10.1007/s00382-022-06363-5.

[18] Muhammad, N.S.; Abdullah, J.; Julien, P.Y. Characteristics of Rainfall in Peninsular Malaysia. In *Journal of Physics: Conference Series*; IOP Publishing: 2022; *1529*, 052014. https://doi.org/10.1088/1742-6596/1529/5/052014.

[19] Wilby, R.L.; Dawson, C.W.; Yu, D.; Herring, Z.; Baruch, A.; Ascott, M.J.; Finney, D.L.; Macdonald, D.M.J.; Marsham, J.H.; Matthews, T.; Murphy, C. Spatial and Temporal Scaling of Sub-Daily Extreme Rainfall for Data-Sparse Places. *Clim. Dyn.* **2023**, *60*(11), 3577–3596. https://doi.org/10.1007/s00382-022-06528-2.

[20] Chenoli, S.N.; Diong, J.Y.; Mohd Nor, M.F.F.; Yip, W.S.; Xavier, P.; Chang, N.K.; Abu Samah, A. Objective Determination of the Winter Monsoon Onset Dates and Its Interannual Variability in Malaysia. *Int. J. Climatol.* **2022**, *42*(16), 10238–10252. https://doi.org/10.1002/joc.7895.

[21] Bohari, N.Z.I.; Saleh, F.Z.; Chang, N.K.; Abdullah, M.F.A. *Review of the Northeast Monsoon 2022/2023 in Malaysia.* Malaysia Ministry of Natural Resources and Environmental Sustainability; Malaysian Meteorological Department: Selangor, Malaysia, 2026; pp. 1–30.

[22] New, X.Y.; Juneng, L.; Tangang, F. Weather Types and Rainfall Variability during the Northeast Monsoon over Malaysia. *PLOS Clim.* **2026**, *5*(6), e0000847. https://doi.org/10.1371/journal.pclm.0000847.

[23] Latos, B.; Ferrett, S.; Lefort, T.; Matthews, A.J.; Lubis, S.W.; Senior, N.V.; Peyrillé, P.; Nguyen, H.; Wheeler, M.C.; Diong, J.Y.; Baranowski, D.B. The Role of Equatorial Waves in Triggering Precipitation Extremes in the Maritime Continent. *Mon. Weather Rev.* **2026**, *154*(3), 333–368. https://doi.org/10.1175/MWR-D-25-0073.1.

[24] Ayoub, A.B.; Juneng, L.; Tangang, F.; Jamaluddin, A.F. MJO Influences on Rainfall Diurnal Cycle during Boreal Summer over Peninsular Malaysia. *Atmos. Res.* **2026**, *339*, 109052. https://doi.org/10.1016/j.atmosres.2026.109052.

[25] Ng, C.K.C.; Sikui, J.J.; Nur Syafiqah, S.K.; Niuls, R. Precipitation Trend and Heterogeneity of Sabah, North Borneo. *Sepilok Bull.* **2019**, *28*, 19–43.

[26] Jamru, L.R.; Jafar, A.; Nadzri, M.I.; Yusoh, M.P.; Cleophas, F. Assessing Satellite Rainfall Accuracy in Dense Tropical Sabah East Coast Forest, Malaysia: A Cross-Validation of Downscaling Technique. *Plan. Malaysia* **2024**, *22*(33), 528–543. https://doi.org/10.21837/pm.v22i33.1566.

[27] Amlan, H.A.; Haniffa, M.R.M.; Allias, N.E.; Muhammad, M.K.I.; Ahmad, M.F.; Zakaria, S.A.A.; Yusop, Z.; Haron, N.A.; Khairuddin, T.K.A. Rainfall Analysis and Hydro-Meteorological Assessment of the November 2024 Flood Event in Kelantan, Malaysia. Preprint.

[28] Yan, H.; Gao, Y.; Wilby, R.; Yu, D.; Wright, N.; Yin, J.; Chen, X.; Chen, J.; Guan, M. Urbanization Further Intensifies Short-Duration Rainfall Extremes in a Warmer Climate. *Geophys. Res. Lett.* **2024**, *51*(5), e2024GL108565. https://doi.org/10.1029/2024GL108565.

[29] Blagojević, J.; Peleg, N.; Prein, A.F.; Marra, F.; Paschalis, A.; Molnar, P. Intensifying Sub-Daily Rainfall Extremes in Tropical Cities: Projections from Downscaled Baselines in a Warming Climate. *Earth's Future* **2026**, *14*(7), e2025EF007703. https://doi.org/10.1029/2025EF007703.

[30] Huffman, G.J.; Stocker, E.F.; Bolvin, D.T.; Nelkin, E.J.; Tan, J. GPM IMERG Final Precipitation L3 Half Hourly 0.1 degree × 0.1 degree V07. Goddard Earth Sciences Data and Information Services Center (GES DISC), Greenbelt, MD, 2023. https://doi.org/10.5067/GPM/IMERG/3B-HH/07.

[31] Japan Aerospace Exploration Agency (JAXA). GSMaP (Hourly). https://doi.org/10.57746/EO.01gs73bkt358gfpy92y2qns5e9.

[32] Lv, P.; Wu, G. The Performance of GPM IMERG Product Validated on Hourly Observations over Land Areas of Northern Hemisphere. *Remote Sens.* **2024**, *16*(22), 4334. https://doi.org/10.3390/rs16224334.

[33] Chang, J.H.W.; Kong, S.S.K.; Sentian, J.; Dayou, J.; Chee, F.P. Synoptic Analysis and Mesoscale Numerical Modelling of Heavy Precipitation: A Case Study of Flash Flood Event in Kota Kinabalu, Malaysia. *Meteorol. Atmos. Phys.* **2020**, *132*(2), 181–201. https://doi.org/10.1007/s00703-019-00682-9.

[34] Mustafah, W.F.; Mokhtar, Z.A.; Abdullah, M.F.A. *Review of the Northeast Monsoon 2024/2025 in Malaysia*. Malaysia Ministry of Natural Resources and Environmental Sustainability; Malaysian Meteorological Department: Selangor, Malaysia, 2025; pp. 1–27.

[35] Davies, P.A.; Fowler, H.J.; Herrera, R.V.; Slingo, J.; Flack, D.L.; Taszarek, M. A New Conceptual Model for Understanding and Predicting Life-Threatening Rainfall Extremes. *Weather Clim. Extrem.* **2024**, *45*, 100696. https://doi.org/10.1016/j.wace.2024.100696.

[36] Elkollaly, M.; Sefelnasr, A.; Sherif, M. A Comprehensive Investigation of Event-Based Rainfall Analysis in Arid and Semi-Arid Climates: An Integration of Innovative Storm Volume-Duration-Frequency (SVDF) Schemes and Event-Based Dimensionless Hyetographs (EDH). *J. Hydrol.* **2025**, *655*, 132959. https://doi.org/10.1016/j.jhydrol.2025.132959.

[37] Pietras, B.; Pyrc, R. Extreme Short-Duration Rainfall and Urban Flood Hazard: Case Studies of Convective Events in Warsaw and Zamość, Poland. *Water* **2025**, *17*(18), 2671. https://doi.org/10.3390/w17182671.

[38] Kang, Y.; Peng, X.; Wang, S.; Hu, Y.; Shang, K.; Lu, S. Observational Analyses of Topographic Effects on Convective Systems in an Extreme Rainfall Event in Northern China. *Atmos. Res.* **2019**, *229*, 127–144. https://doi.org/10.1016/j.atmosres.2019.05.024.

[39] Su, L.; Sun, X.; Du, Y.; Fung, J.C.; Chen, G. The Roles of Local Convergences in the Convection Initiation of a Record-Breaking Rainfall Event at the Coastal Pearl River Delta in South China. *J. Geophys. Res. Atmos.* **2023**, *128*(3), e2022JD037234. https://doi.org/10.1029/2022JD037234.

[40] Wu, S.N.; Sakaeda, N.; Martin, E.; Rios-Berrios, R.; Russell, J. The Contribution of Mesoscale Convective Systems to the Coastal Rainfall Maximum over West Africa. *Mon. Weather Rev.* **2024**, *152*(8), 1787–1802. https://doi.org/10.1175/MWR-D-23-0148.1.

[41] Qian, J.H.; Robertson, A.W.; Moron, V. Diurnal Cycle in Different Weather Regimes and Rainfall Variability over Borneo Associated with ENSO. *J. Clim.* **2013**, *26*(5), 1772–1790. https://doi.org/10.1175/JCLI-D-12-00178.1.

[42] Wei, Y.; Pu, Z.; Zhang, C. Diurnal Cycle of Precipitation over the Maritime Continent under Modulation of MJO: Perspectives from Cloud-Permitting Scale Simulations. *J. Geophys. Res. Atmos.* **2020**, *125*(13), e2020JD032529. https://doi.org/10.1029/2020JD032529.

[43] Hanifa, R.; Wiratmo, J. ENSO and IOD Influence on Extreme Rainfall in Indonesia: Historical and Future Analysis. *Agromet* **2024**, *38*(2), 78–87. https://doi.org/10.29244/j.agromet.38.2.78-87.

[44] Senior, N.V.; Matthews, A.J.; Webber, B.G.; Paski, J.A.; Nuryanto, D.E.; Jones, R.W.; Permana, D.S.; Febriyanti, A.A.H. Abrupt Ending of the Madden–Julian Oscillation by Convectively Coupled Kelvin Wave Precipitation Leaves a Swath of Flooding across Indonesia. *Q. J. R. Meteorol. Soc.* **2025**, *151*(771), 4997. https://doi.org/10.1002/qj.4997.

[45] Bayhaqi, A.; Iskandar, M.R.; Azminuddin, F.; Mubarrok, S.; Iqbal, M.; Surinati, D.; Abdullah, F.A.R. Historical Characteristics and Climate Mode Modulation of Extreme Wave Climate over Indonesian Maritime Continent Based on ERA5

Reanalysis Data. *Clim. Dyn.* **2026**, *64*(5), 229. https://doi.org/10.1007/s00382-026-08204-1.

[46] Fakaruddin, F.J.; Yip, W.S.; Diong, J.Y.; Dindang, A.K.; Chang, N.; Abdullah, M.H. Occurrence of Meridional and Easterly Surges and Their Impact on Malaysian Rainfall during the Northeast Monsoon: A Climatology Study. *Meteorol. Appl.* **2019**, *27*(1), e1836. https://doi.org/10.1002/met.1836.

[47] Yin, X.; Zhang, Z.; Lin, Z.; Yin, J. Assessment of Rainfall Frequencies from Global Precipitation Datasets. *Atmosphere* **2025**, *16*(1), 66. https://doi.org/10.3390/atmos16010066.

[48] Parsons, D.; Stern, D.; Ndanguza, D.; Sylla, M.B.; Musyoka, J.; Bagiliko, J.; Clarkson, G.; Dorward, P. Evaluating Satellite and Reanalysis Rainfall Estimates for Climate Services in Agriculture: A Comprehensive Methodology. *Meteorol. Appl.* **2026**, *33*(2), e70170. https://doi.org/10.1002/met.70170.

[49] Hayashi, Y.; Tebakari, T.; Hashimoto, A. A Comparison between Global Satellite Mapping of Precipitation Data and High-Resolution Radar Data—A Case Study of Localised Torrential Rainfall over Japan. *J. Disaster Res.* **2021**, *16*(4), 786–793. https://doi.org/10.20965/jdr.2021.p0786.

[50] Liu, S.; Wang, J.; Wang, H. Analysis of the Monitoring Ability of High-Resolution Satellites for the "21·7" Heavy Rain in Henan. *Acta Meteorol. Sin.* **2022**, *80*(5), 765–776. https://doi.org/10.11676/qxxb2022.053.

[51] Chen, H.; Liu, X.; Gao, Y.; Wang, H.; Yang, H. Comparison Analysis of Thirteen Global Precipitation Datasets over Mainland China. *Remote Sens.* **2026**, *18*(10), 1459. https://doi.org/10.3390/rs18101459.

[52] Kachi, M.; Aonashi, K.; Kubota, T.; Shige, S.; Ushio, T.; Mega, T.; Yamamoto, M.; Hamada, A.; Seto, S.; Takayabu, Y.N.; Oki, R. Developments and Applications of the Global Satellite Mapping of Precipitation (GSMaP) for the Global Precipitation Measurement (GPM). *Geophys. Res.* **2016**, *18*, 11384.

[53] Huffman, G.J.; Bolvin, D.T.; Braithwaite, D.; Hsu, K.L.; Joyce, R.J.; Kidd, C.; Nelkin, E.J.; Sorooshian, S.; Stocker, E.F.; Tan, J.; Wolff, D.B. Integrated Multi-Satellite Retrievals for the Global Precipitation Measurement (GPM) Mission (IMERG). In *Satellite Precipitation Measurement*; Volume 1; Springer International Publishing: Cham, Switzerland, 2020; pp. 343–353.

[54] Xu, J.; Ma, Z.; Yan, S.; Peng, J. Do ERA5 and ERA5-Land Precipitation Estimates Outperform Satellite-Based Precipitation Products? A Comprehensive Comparison between State-of-the-Art Model-Based and Satellite-Based Precipitation Products over Mainland China. *J. Hydrol.* **2022**, *605*, 127353. https://doi.org/10.1016/j.jhydrol.2021.127353.

[55] Lv, X.; Guo, H.; Tian, Y.; Meng, X.; Bao, A.; De Maeyer, P. Evaluation of GSMaP Version 8 Precipitation Products on an Hourly Timescale over Mainland China. *Remote Sens.* **2024**, *16*(1), 210. https://doi.org/10.3390/rs16010210.

[56] Da Silva, N.A.; Webber, B.G.; Matthews, A.J.; Feist, M.M.; Stein, T.H.; Holloway, C.E.; Abdullah, M.F. Validation of GPM IMERG Extreme Precipitation in the Maritime Continent by Station and Radar Data. *Earth Space Sci.* **2021**, *8*(7), e2021EA001738. https://doi.org/10.1029/2021EA001738.

[57] Weng, P.; Tian, Y.; Jiang, Y.; Chen, D.; Kang, J. Assessment of GPM IMERG and GSMaP Daily Precipitation Products and Their Utility in Drought and Flood Monitoring across Xijiang River Basin. *Atmos. Res.* **2023**, *286*, 106673. https://doi.org/10.1016/j.atmosres.2023.106673.

[58] Sharma, S.; Evans, J.P.; Pitman, A.; Behrangi, A. Urban Rainfall Trends in IMERG Datasets. *Environ. Res. Lett.* **2026**, *21*(11), 114017. https //doi.org/10.1088/1748-9326/ae7135.

[59] Ding, M.; Zheng, X.T.; Li, D.; Li, Z.; Chen, H.; Sun, T. Global Urban-Rural Differences in Precipitation: Cities See More Light Rain but Milder Extremes. *Earth's Future* **2026**, *14*(4), e007370. https //doi.org/10.1029/2025EF007370.

[60] Wu, L.; Ren, Y.; Huang, P.; Yuan, S.; Zhou, C.; Gu, Z.; Guo, Y.; Zhou, L. Evaluation of GSMaP and MSWEP Precipitation Products for Runoff Simulation in the Lhasa River Basin. *PLoS ONE* **2026**, *21*(2), e0342995. https //doi.org/10.1371/journal.pone.0342995.

[61] Rajeev, A.; Masleyev, M.A.; Pendergrass, A.G. Dependence of the Precipitation Intensity Distribution on Spatial and Temporal Resolution in Observations. Preprint, 2026.

[62] Conte, L.C.; Tassi, R.; Bayer, D.M. Satellite-Based Rainfall Datasets: A Global Systematic Review of Applications, Accuracy, and Research Gaps. *IEEE Access* **2026**, *14*, 29539–29565. https //doi.org/10.1109/ACCESS.2026.3667060.